Sixth International Symposium on Turbulence and Shear Flow Phenomena
Seoul, Korea, 22-24 June 2009

MRV ENABLED CFD FOR TURBINE INTERNAL COOLING FLOW

Christopher J. Elkins, Marcus Alley, John K. Eaton
Department of Mechanical Engineering
Stanford University
488 Escondido Mall, Bldg 500, Stanford, CA 94305
celkins@stanford.edu, mtalley@stanford.edu, eatonj@stanford.edu

Frank Mignano, Ardeshir Riahi
Honeywell Aerospace, Turbo and Rotating Machinery Department
111 South 34th Street , Phoenix, Arizona 85034
frank.mignano@honeywell.com, ardeshir.riahi@honeywell.com

ABSTRACT

The full three-dimensional three-component velocity field in a scaled model of the complete internal cooling circuit of a typical gas turbine blade is measured experimentally with Magnetic Resonance Velocimetry (MRV) and compared with CFD results using FLUENT with four different turbulence models: k-ε, v2f, k-ω, and Spalart-Allmaras and CFX with the k-ε model. Both the FLUENT and CFX with k-ε results best agreed with the MRV data. All three of these datasets are directly compared in cross planes throughout the geometry including zones in the leading edge with jet impingement, the bend of a ribbed serpentine passage, and the pin fin arrays in the trailing edge. The CFX predictions agreed reasonably well with the experimental MRV results for most regions of the flow. FLUENT did not perform as well, particularly in the regions of the blade dominated by separation which include the cross-over holes in the leading edge passage, the serpentine bend, and the cylindrical pin fins. This combined experimental/computational program shows the utility of rapid prototyping experiments as an adjunct to CFD.

INTRODUCTION

Internal cooling flows for turbine blades and vanes are extremely challenging to analyze and design. The flow geometry is highly complex, and it is impossible to obtain experimental information about the flow under actual operating conditions. Three dimensional CFD is the obvious choice for design calculations, but the accuracy of such calculations is dependent on the choice of turbulence model, numerical scheme, gridding, and boundary conditions. Magnetic Resonance Velocimetry (MRV) can provide 3-D data sets in arbitrarily complex geometries in non-rotating, isothermal conditions for CFD validation. Once validated, useful quantities such as pressures and wall shear stresses can be obtained from the CFD results. Moreover, computations can be performed under more realistic operating conditions with confidence in the results.

The internal cooling system in a turbine blade is typically broken into three regions: a leading edge passage with jet impingement, mid-blade ribbed serpentine passages, and a trailing edge passage with pin fin arrays (Iacovides and Launder 2007). Figure 1 shows a generic sketch of the typical internal cooling layout. The turbine blade internal cooling literature is extensive with studies typically focusing on the aerodynamic and thermal performance in one of the three regions. The purpose of this paper is not to review internal cooling in blades. The interested reader is directed to recent articles: Iacovides and Launder (2007) discuss all three regions, Taslim and Bethka (2009) investigate leading edge cooling with jet impingement, Han and Chen (2006) consider ribbed serpentine passages, and Cunha and Chyu (2006) cover trailing edge cooling.

MRV methods are described in detail in Elkins and Alley (2007). Iaccarino and Elkins (2006) present a study of the flow through square, ribbed, serpentine passages in which CFD results are compared with experimental measurements from particle image velocimetry (PIV) and MRV. They show that the experimental MRV results complement CFD results in identifying critical regions of interest for improving the numerical calculations and the aerodynamic performance of the passages.

Few previous studies, if any, have investigated the entire internal cooling geometry. This can be important in order to capture the interdependence among the three regions since middle serpentine passages often feed coolant to the leading edge and/or trailing edge passages. The present study investigates the complete internal cooling flow field in a turbine blade using the combination of CFD and MRV. The investigated cooling system includes leading edge jet impingement cooling with local extraction via film cooling holes, ribbed serpentine passages in the middle of the blade, and pin fin arrays in the aft portion of the blade. The overall objectives of the program are to observe the basic characteristics of the flow field including regions with high pressure losses and poor heat transfer and to validate CFD results for non-rotating and isothermal flow conditions.

METHODS

Flow Model

A 7X scale flow model of a typical turbine blade was created in CAD. The model included the full geometry of

the internal cooling passages and the film cooling holes in the blade surface. An inlet manifold was added to the CAD model to distribute fully developed pipe flow into the blade's four passage inlet to provide simple inlet condition specification for the CFD. Figure 2 shows the geometry of this manifold as it transitions from the circular pipe to the four inlet passages. Exit manifolds were also added to the CAD model and placed around groups of film cooling holes at the surface of the blade. These groups include leading edge shower head film holes, suction side film holes, tip cap holes, and the trailing edge holes are split into two groups. The manifolds have linearly increasing cross-sectional area along their length in order to create an approximately uniform outlet pressure condition for the film cooling holes exhausting into each manifold. The flow rates through each of the exit manifolds were adjusted using valves in order to match flow conditions measured in an ambient air experiment in a different scale model with the same geometry. The CAD model was accurately manufactured using steroelithography (SLA), so both the measurements and computations were based on the same geometry.

Gadolinium doped water (concentration of 0.5% by volume) was circulated through the model at a flow rate of 41.6 l/min. The Reynolds number based on bulk mean velocity and pipe diameter for the inlet pipe flow was 19,300.

Magnetic Resonance Velocimetry (MRV)

The full three-dimensional velocity field was measured in a 1.5T MR system (GE Signa CV/I, G_{max} = 50mT/m, rise time = 268μs) using the phase-contrast MRV method described in Elkins et al. (2003) modified to scan without the cine MRI functionality. The model was scanned inside a single channel receive coil designed for human heads. The measurement domain contained the 4 inlet passages of the original blade design, the internal passages of the blade, and the 6 exit manifolds. The measured domain was 20 cm in the blade height direction by 24 cm by 24 cm in the other directions with a resolution of 1.0 mm by 0.9 mm by 0.9 mm, respectively. The full field of velocities was measured 8 times, and these were averaged to produce the final data set. The spatial resolution of the MRV measurements was sufficient to allow direct point by point comparison with the CFD.

CFD

A hybrid computational mesh was created using GAMBIT 2.2 for the 7X scale model. Cylindrical extensions 3 diameters long were added to the exit manifolds and 4 diameters long to the inlet to simulate the straight exit and inlet tubes used in the experimental flow model. A Cooper mesh was used in all of these extensions. A tetrahedral mesh was used for the remaining interior of the model. In total, 4.8 million cells were used with a range in wall normal resolution corresponding to y^+=1-20. The mesh was of high quality having less than 0.93 skewness.

The flow field and the turbulence characteristics were computed with water at 70 °F using FLUENT with four different turbulence models: k-ε, v2f, k-ω, and Spalart-Allmaras. An additional calculation was done using CFX and the k-ε model. The inlet mass flow rate matched the experiment with the inlet Re_D=19,300, and the inlet profile was prescribed as 1D. The exit boundary conditions were determined in the following way. A preliminary FLUENT (k-ε) computation was done with the flow rates in the 6 exit manifolds prescribed to match those in the experiment. Again, 1D profiles were used. The exit pressure and turbulence quantity profiles were taken from this simulation and used for the exit boundary conditions for all subsequent computations. The results using FLUENT with k-ε and CFX with k-ε showed the best agreement with the MRV, and these are the CFD cases presented in this paper.

RESULTS

The inlet condition to the model was fully developed pipe flow at a Reynolds number equal to 19,300. Table 1 lists the percentage differences between the flow rates in each exit manifold for the MRV versus each CFD case. The data from the two trailing edge exit manifolds are grouped into the last column. Most of the differences are less than +/-5%. The largest differences are seen in the tip cap.

The MRV results were rotated and translated into the CFD coordinate system for direct comparison. The average velocity distributions in the passages of the blade can be measured and compared by integrating the flow through cross planes in the passages. Figure 3 shows the average radial velocities in the four inlet passages for the MRV, FLUENT with k-ε, and CFX with k-ε results. Note that the combined flowrate through all four channels agree to within 2%, but the distribution among the four channels varies significantly. The distribution for the CFX results agrees well with the MRV, but the FLUENT results show differences of as much as 26% in the bottom channel. Similarly, the flow rates through horizontal cross planes positioned every 20 mm along the entire height of the blade were calculated, and the agreement for all cases is excellent with the error varying between 0.2% and 3.5%. However, as seen in figure 3, the distribution in specific passages can vary significantly. Moreover, the actual flow patterns within passage cross sections vary. Since it is the distribution of the flow within the passages that determines the heat transfer and the cooling of the blade, these patterns will be the focus of the remainder of the results.

The leading edge passage contains jet impingement cooling created by race-track shaped cross-over holes. Figures 4 and 5 show contours of velocity magnitude in planes of data extracted from the leading edge crossover holes and the leading edge passage, respectively. In Figure 4, the MRV and CFX (k-ε) results compare well in terms of velocity magnitude and flow patterns. For instance, the separation regions in the lower left corners of the cross-over holes are similar. When the results are compared in a different plane that includes the crossover holes and the leading edge passage (Figure 5), the FLUENT (k-ε) results mispredict the flow patterns while the CFX (k-ε) results are in better agreement with the MRV results.

Figure 6 is a vector plot showing the bottom two cross-over jets in a plane with its vertical and horizontal axes through the centers of the jets. The vector plot shows clearly the impingement zones on the leading edge passage wall

and the circulation zones between the two jets. In this centered plane which is slightly different from the plane in Figure 5, FLUENT captures the shape of the jets and the velocity magnitudes better than CFX.

The middle of the blade is cooled by ribbed passages with serpentine bends. These passages have strong secondary flows combined with flow separation at the bends. Figure 7 shows two vertical cross planes cutting through a downward (toward the hub) passage. The left images show the passage center, and the right show a plane close to the suction side wall. Two ribs on this wall are evident. CFX better predicts the flow separation at the bend and its development along the suction side wall. Contrary to MRV and CFX, FLUENT shows the flow reattaching on the suction side wall at the start of the second rib.

Figure 8 contains three horizontal cross planes in the same passage to illustrate the development of the large separated region beginning at the bend and extending along the suction side wall. The MRV and CFX results show a similar separation at the bend and the two downstream positions. FLUENT shows very different flow at the bend and at the most downstream plane. While FLUENT seems to predict the peak velocity magnitudes well, it performs poorly in the separated regions.

The aft portion of the blade contains an array of pin fins. Figure 9 shows velocity vectors shaded by velocity magnitude in the flow around a central region of the pin fin array. Recirculation zones are evident in the dark regions behind the pin fins. Note also that the flow is accelerating as it approaches the trailing edge due to the narrowing of the blade. Compared to the MRV and CFX, the FLUENT results show higher velocities in the local regions around the tops and bottoms of the cylinders. Again, the CFX velocities are slower than the MRV.

Figure 10a is a plot of the velocity along a vertical line through the data shown by Figure 9. The streamwise position of this line is indicated by the vertical white line in Figure 9. Note that the negative peak velocities in the recirculation regions are about 10-20% of the peak velocities between the fins. The MRV and CFX data agree qualitatively well but disagree in the peak velocities between the pin fins. Part of this error is due to slight misalignment between the two data sets. It also appears that the CFX results show a broader but slower velocity profile between the pin fins. This may indicate that the CFX is missing the separation point on the cylindrical pin fin slightly. The FLUENT results show larger qualitative and quantitative differences. The main differences are in the sizes of the wakes behind the pin fins and the absence of negative velocities in these regions. This indicates FLUENT is miscalculating the separation and shear layer development around the pin fins.

Figure 10b is a plot of velocity along a streamwise line through the centers of the pin fins. The vertical position of this line is indicated by the horizontal white line in Figure 9. This plot clearly shows the overall acceleration of the flow as it approaches the trailing edge as well as the presence of recirculation regions. The MRV and CFX results show good agreement although the peak velocities differ. FLUENT does not capture the recirculation behind the pin fins.

DISCUSSION

The presentation of the results highlights the three-dimensionality and complexity of the internal flow in a gas turbine blade. Full field information in such flows is not realistically achievable with experimental methods other than MRV. MRV makes it possible to obtain 3D information quickly. For example, this experiment took 2 weeks from start of manufacturing to completion of data analysis. The bulk of the time is taken by the SLA manufacturing process, and the experiments themselves require only 3-4 hours.

The results surveyed three regions of the blade cooling system and illustrated significant differences between two CFD codes which both used the k-ε model. The experimental data allows determination of which code is better suited for the specific geometry. MRV gives the blade designer velocity data by which to validate the CFD results in the actual blade geometry for simple laboratory conditions such as no rotation and no compressibility. Once confidence is established in the simple computations, more realistic complexity can be added to the simulations for further evaluation of blade performance.

CONCLUSIONS

We created a scaled model of the internal cooling passages of a typical high pressure turbine blade and performed a joint experimental and computational study of the internal flow using MRV, FLUENT with k-ε, v2f, k-ω, and Spalart-Allmaras turbulence models, and CFX with k-ε. The FLUENT and CFX results using the k-ε model showed the best agreement with the MRV, and these three datasets were compared directly in the major regions of the blade, namely, the leading edge passage with jet impingement, the middle ribbed serpentine passages, and the trailing edge pin fin array. The CFX results agreed best with the MRV data, particularly in regions with complex flow dominated by separation and secondary flows. FLUENT performed less well in predicting flow separation specifically in the serpentine passages and the pin fin array.

Table 1: Percentage differences between the flow rates in each exit manifold for the MRV versus each CFD case.

	LE Shower-head	Suction Side Film	Tip Cap	Trailing Edge
k-e	-4%	1%	5%	-1%
v2f	-5%	-5%	4%	3%
kw	-3%	2%	2%	1%
CFX	-1%	0%	9%	-6%

REFERENCES

Cunha, F.J. and Chyu, M.K., 2006, "Trailing-edge cooling for gas turbines", *J. Propulsion and Power*, Vol.22, iss.2, p.286-300.

Elkins, C.J., Markl, M., Pelc, N. and J.K. Eaton, 2003, "4D Magnetic Resonance Velocimetry for Mean Velocity Measurements in Complex Turbulent Flows", *Experiments in Fluids*, 34, 494-503.

Elkins, C. J., M. Alley, 2007, "Magnetic Resonance Velocimetry: Applications of Magnetic Resonance Imaging in the Measurement of Fluid Motion", *Exp. in Fluids*, 43:823-858.

Fu, W.L., Wright, L. M., and Han, J.C., 2005, "Heat transfer in 2-pass rotating rectangular channels with smooth wall", *ASME J. Heat Transf.*, 127, 265–277.

Han, J.C. and Chen, H.C., 2006, "Turbine blade internal cooling passages with rib turbulators", *J. Propulsion and Power*, Vol.22, iss.2, p.226-248.

Iaccarino, G. and C. Elkins, 2006, "Towards rapid analysis of turbulent flows in complex internal passages", *Flow Turbulence Combust*, 77: 27-39.

Iacovides, H. and Launder, B.E., 2007, "Internal blade cooling: the Cinderella of computational and experimental fluid dynamics research in gas turbines", *Proceedings of the Institution of Mechanical Engineers, Part A: J. Power and Energy*, Vol.221, iss.3, p.265-290.

Taslim, M.E. and Bethka, D., 2009, "Experimental and numerical impingement heat transfer in an airfoil leading-edge cooling channel with cross-flow", *J. of Turbomachinery*, vol:131 iss:1 pgs:011021-1 thru 011021-7.

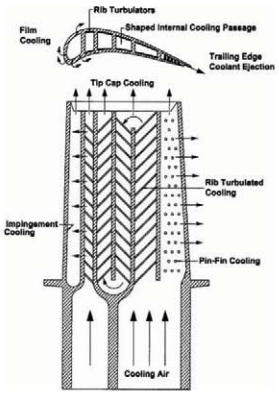

Figure 1: Schematic showing the typical internal cooling passages of a turbine blade including jet impingement in the leading edge passage, ribbed serpentine passages in the middle of the blade, and pin fin cooling in the trailing edge passage (Fu et al. 2005).

Figure 2: Picture showing the entrance manifold which changes from a circular pipe to the four large aspect ratio channels typically found in turbine blades.

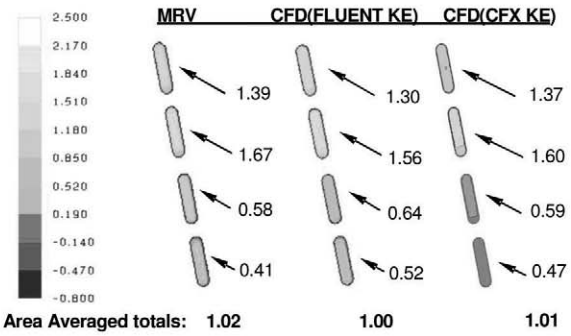

Figure 3: Comparison of the area averaged velocities (m/s) in the four inlet channels for the MRV, FLUENT k-ε, and CFX k-ε results.

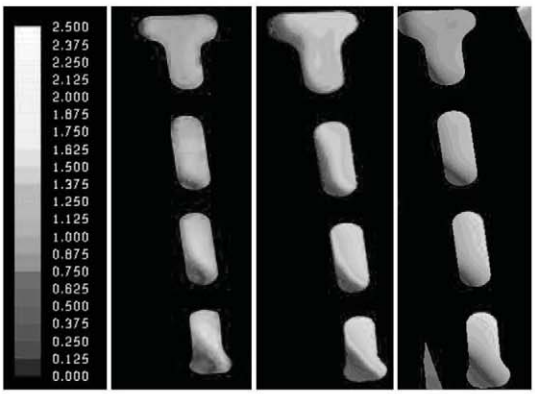

Figure 4: Velocity magnitude contours in a vertical slice through the race track shaped crossover holes feeding the leading edge passage. Note the separation regions in the corners of the holes agree between the MRV (left), FLUENT k-ε (mid) and CFX k-ε (right).

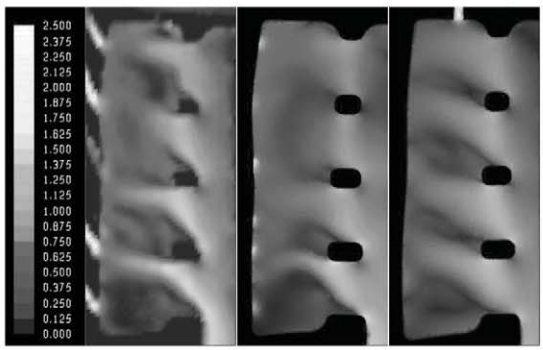

Figure 5: Velocity magnitude contours showing flow through cross over holes impinging on the inside of the leading edge. The MRV (left) results agree better with CFX k-ε (right) than FLUENT k-ε (middle).

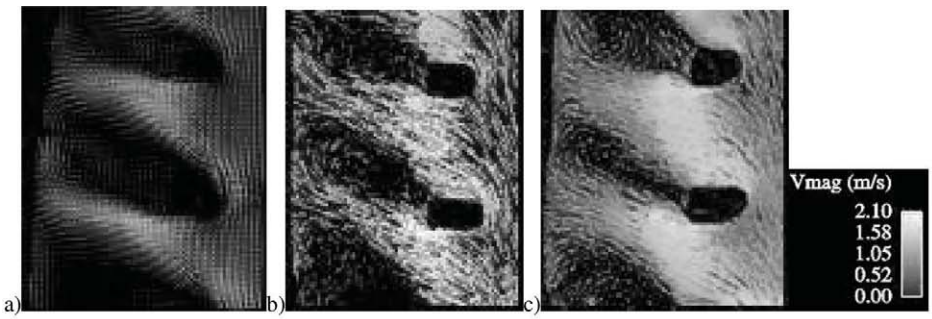

Figure 6: Velocity vector plots (MRV (a), FLUENT k-ε (b), CFX k-ε (c)) showing the bottom two cross-over jets in a plane with its vertical and horizontal axes through the centers of the jets. Grayscale levels indicate velocity magnitude (m/s).

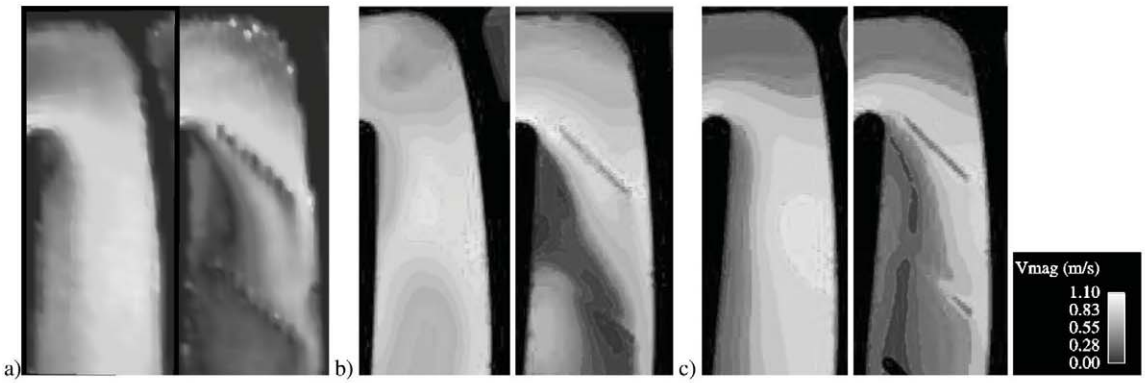

Figure 7: Contour plots of velocity magnitude (MRV (a), FLUENT k-ε (b), CFX k-ε (c)) in two vertical cross planes cutting through a downward serpentine passage: passage center (left) and close to the suction side (right). Note the influence of the ribs on the suction side in the right side pictures.

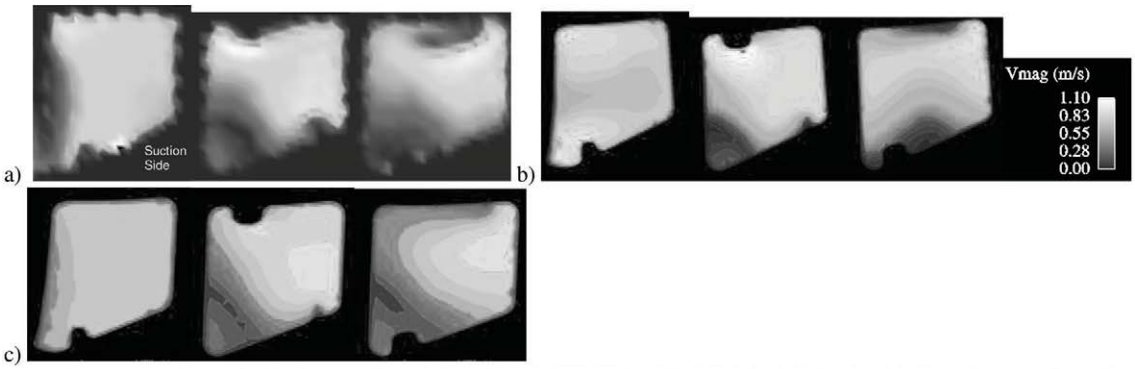

Figure 8: Contour plots of velocity magnitude (MRV (a), FLUENT k-ε (b), CFX k-ε (c)) in three horizontal cross planes in the same passage shown in Figure 7. The suction side wall is labeled. The left image is placed near the 180 degree bend, the middle is placed at the downstream end of the first rib, and the right is placed at the start of the second rib. Both ribs are evident in the right side images in Figure 7.

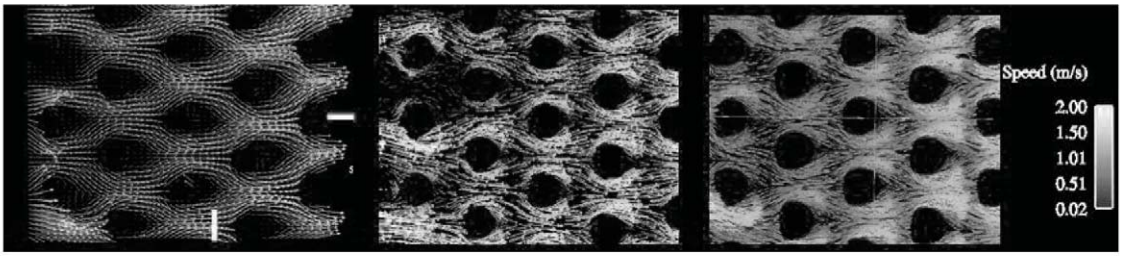

Figure 9: Velocity vector plots (MRV (a), FLUENT k-ε (b), CFX k-ε (c)) in the center plane of a region of the pin fin array. Grayscale levels indicate velocity magnitude. White lines indicate the positions of the axes used in Figure 10.

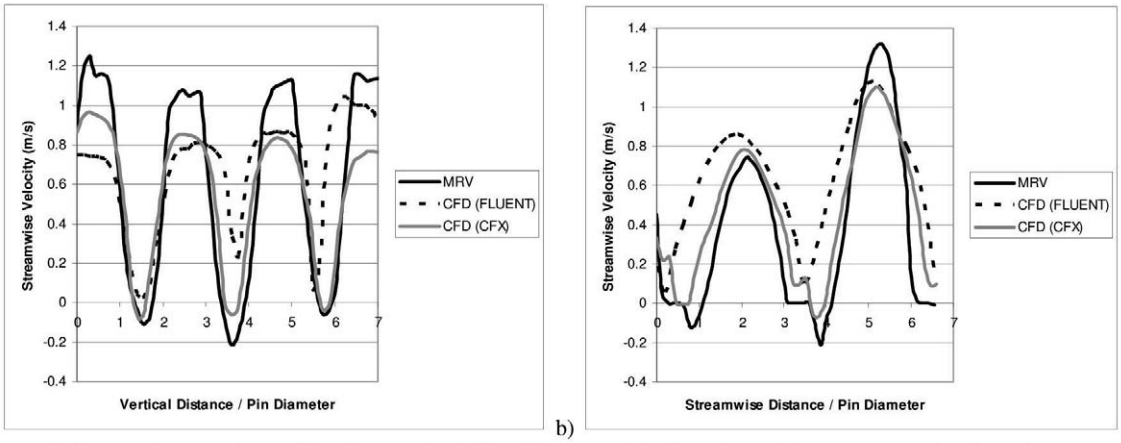

a) b)

Figure 10: Streamwise velocity profiles along vertical (a) and horizontal (b) lines through the data shown by Figure 9.